JOURNAL OF BACTERIOLOGY, Oct. 1991, p. 5935–5943
0021-9193/91/195935-09$02.00/0

Vol. 173, No. 19

Dimethyl Sulfoxide Reductase of *Escherichia coli*: an Investigation of Function and Assembly by Use of In Vivo Complementation

D. SAMBASIVARAO AND JOEL H. WEINER*

Department of Biochemistry, University of Alberta, Edmonton, Alberta, Canada T6G 2H7

Received 5 June 1991/Accepted 22 July 1991

Dimethyl sulfoxide (DMSO) reductase of *Escherichia coli* is a membrane-bound, terminal anaerobic electron transfer enzyme composed of three nonidentical subunits. The DmsAB subunits are hydrophilic and are localized on the cytoplasmic side of the plasma membrane. DmsC is the membrane-intrinsic polypeptide, proposed to anchor the extrinsic subunits. We have constructed a number of strains lacking portions of the chromosomal *dmsABC* operon. These mutant strains failed to grow anaerobically on glycerol minimal medium with DMSO as the sole terminal oxidant but exhibited normal growth with nitrate, fumarate, and trimethylamine *N*-oxide, indicating that DMSO reductase is solely responsible for growth on DMSO. In vivo complementation of the mutant with plasmids carrying various *dms* genes, singly or in combination, revealed that the expression of all three subunits is essential to restore anaerobic growth. Expression of the DmsAB subunits without DmsC results in accumulation of the catalytically active dimer in the cytoplasm. The dimer is thermolabile and catalyzes the reduction of various substrates in the presence of artificial electron donors. Dimethylnaphthoquinol (an analog of the physiological electron donor menaquinone) was oxidized only by the holoenzyme. These results suggest that the membrane-intrinsic subunit is necessary for anchoring, stability, and electron transport. The C-terminal region of DmsB appears to interact with the anchor peptide and facilitates the membrane assembly of the catalytic dimer.

Dimethyl sulfoxide (DMSO) reductase catalyzes the final step of an energy-transducing anaerobic electron transport chain in *Escherichia coli* (3, 4). The enzyme catalyzes the reduction of DMSO, trimethylamine *N*-oxide (TMAO), and a number of *S*- and *N*-oxide compounds (33) but is genetically distinct from other TMAO reductases in *E. coli* (5). The membrane-bound enzyme has been purified to homogeneity (33); the *dms* operon, coding for DMSO reductase, has been cloned (4), and its DNA sequence has been determined (2). It is an iron-sulfur molybdoenzyme composed of three nonidentical subunits in equimolar ratio. The large 87,350-Da DmsA subunit is homologous to a number of molybdopterin-containing proteins, binds this cofactor, and is involved in the catalytic function. A 23,070-Da DmsB subunit contains 16 cysteine residues arranged in four groups. These groups bear homology to the iron-sulfur center binding sequences of the (4Fe-4S) ferredoxins (2) and serve to coordinate the electron transfer centers (8). Hydrophobicity analysis of the DmsC subunit (30,789 Da), using the Kyte-Doolittle algorithm (14), indicates that it is composed of eight hydrophobic segments of appropriate length to cross the *E. coli* plasma membrane in an α-helical configuration, and we have proposed that this polypeptide anchors the hydrophilic DmsAB subunits to the cytoplasmic surface of the membrane (2, 25). However, the physiological role of DMSO reductase in anaerobic respiration remains obscure. The occurrence of multiple reductases in *E. coli* (35) complicated the study and necessitated the construction of a bank of deletion and disruption mutants in the structural genes of DMSO reductase. These mutants enabled us to study the functions of individual subunits without interference from the chromosomally encoded wild-type DMSO reductase.

We monitored the expression and properties of DMSO reductase encoded by multicopy plasmids carrying *dms* genes singly or in combination. Using this method of in vivo complementation, we demonstrated that DMSO reductase is the only enzyme in *E. coli* that is capable of utilizing DMSO under anaerobic growth conditions. A comparison of the DMSO- and TMAO-reducing activities from the wild type and the *dms* deletion strain grown anaerobically in the absence of inducers clearly established that DMSO reductase and the previously described constitutive TMAO reductase (1) are one and the same.

MATERIALS AND METHODS

Chemicals and reagents. Benzylviologen (BV), dithiothreitol (DTT), TMAO, and 3-(*N*-morpholine)propane sulfonic acid (MOPS) were obtained from Sigma Chemical Co., St. Louis, Mo. DMSO was obtained from Fisher Scientific Ltd., Edmonton, Alberta, Canada. Dimethylnaphthoquinone (DMN) was a gift of A. Kroger, J. W. Goethe University, Frankfurt, Germany. Electrophoretic apparatus and reagents for immunoblotting were obtained from Bio-Rad Laboratories, Richmond, Calif. All other chemicals were of the highest grade commercially available.

Construction of recombinant plasmids. The various strains and plasmids used are summarized in Tables 1 and 2. These can be categorized as follows.

(i) Plasmids carrying the entire *dms* operon. pLC 19-36 was isolated from the Clarke-Carbon plasmid bank and carries the entire *dms* operon and the flanking regions on the chromosome (Fig. 1) (5). Plasmids pDMS159, pDMS216, and pDMS229 carrying the entire *dms* operon were described earlier (5). These plasmids were chosen for further subcloning experiments since they (on various vector backgrounds) provided convenient restriction sites. A 6.5-kb *Sal*I fragment (*dmsABC*) was isolated from pDMS216 and ligated into the *Sal*I site of pACYC186 to yield pDMS240.

(ii) Construction of plasmids carrying deletions or insertions in the *dms* operon. Digestion and subsequent ligation of

* Corresponding author.

TABLE 1. Strains

Strain	Genotype	Source
TG1	Δ(*lac-pro*) *supE thi hsdD5*/ F′ *traD36 proA*$^+$*B*$^+$ *lacI*^{q} *lacZ*ΔM15	Laboratory collection
DSS106	As TG1; Km^r Δ*dmsA-dmsBC*	This work
DSS108	As TG1; Km^r *dmsAB′-dmsC*	This work
DSS301	As TG1; Km^r Δ*dmsABC*	This work
JC7623	*thr-1 ara-14 leuB6* Δ(*proA2*) *lacY1 sbcC201 tsx-33 supE44 galK2* λ$^-$ *sbcB15 hisG4 recB21 recC22 rpsL31 xyl-5 mtl-1 argE3 thi-1*	R. B. Gennis, University of Illinois

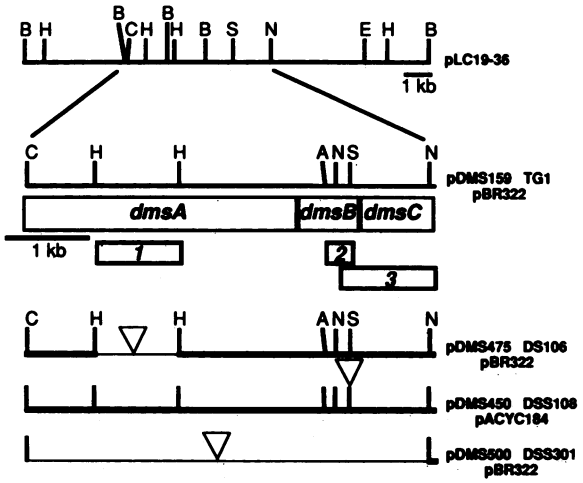

FIG. 1. Schematic representation of the construction of the normal and mutant recombinant plasmids carrying the *dmsABC* genes. Plasmids pLC19-36 and pDMS159 were described earlier (5). Insertions or deletions in *dms* genes were carried out as described in Materials and Methods. The various *dms* plasmids used, the derived mutant strains, and the vector are identified at the right of each linearized plasmid. Thick continuous horizontal bars denote the wild type *dms* operon. The regions spanning the *dmsA*, *-B*, and *-C* genes are identified individually in boxed regions. The DNA fragments used as probes (^{32}P labelled) for Southern blot analysis were numbered sequentially in the boxed regions below the respective genes. The thin lines interrupting the bars represent deletions, and each inverted triangle represents an insertion of the 1.6-kb kanamycin resistance cartridge. Note that the pDMS159 map is truncated at the end of the *dmsC* gene, and only the sequences upstream of the *dms* operon up to the *Cla*I site are shown for convenience. Restriction endonuclease sites: A, *Ava*I; B, *Bam*HI; C, *Cla*I; E, *Eco*RI; H, *Hin*dIII; N, *Nde*I; S, *Sac*I.

pDMS159 with *Hin*dIII deleted a 1.0-kb region in *dmsA* with and without the 1.6-kb kanamycin cartridge (derived from pUC4-KIXX) resulted in plasmids encoding the DmsB and C subunits, pDMS475 (Fig. 1) and pDMS350, respectively. pDMS240 has a unique *Sst*I site in *dmsB*, 90 nucleotides upstream of *dmsC*. Insertion of the 1.6-kb kanamycin cartridge derived from pUC4-KIXX at this site created pDMS450 (Fig. 1). Digestion of pDMS229 by *Sst*I resulted in a fragment carrying *dmsAB′* and deleted in *dmsC*. Upon insertion into the *Sst*I site of pACYC184, this fragment resulted in pDMS355. Plasmid pDMSC59 carries the alkaline phosphatase gene (*phoA*) fused to *dmsC* at Leu-76 (Fig. 2). Gene fusions were generated by infecting *E. coli* CC118/ pDMS159 with λ TnPhoA as described earlier (25). Alkaline phosphatase fusions were mapped by restriction enzyme digestions and by DNA sequence analysis (26). The fusion plasmid pDMSC59, was stabilized by deleting the *Xho*I fragment from the 3′ end of the transposon. The resulting plasmid, pDMSC59X, carries full *dmsAB* and the coding region of *phoA*. Plasmid pDMS500, generated by *Hin*dIII digestion of pDMSC59 (Fig. 2), lacks the entire *dms* operon.

Construction of mutant strains defective or deleted in the chromosomal *dms* operon. The method of homologous recombination was adopted for the construction of various mutants, using a *recBC sbc* strain as described previously (12). The plasmids carrying kanamycin and ampicillin or chloramphenicol resistance markers and altered or deleted in *dms* genes were introduced into *E. coli* JC7623 by transformation (18). The plasmids cannot replicate in this strain, and the Km^r marker was rescued by site-specific recombination and selection on kanamycin-containing medium. Colonies which were kanamycin resistant and ampicillin or chloramphenicol sensitive alone had the correct mutation as assessed by Southern blot analysis (Fig. 3). These mutations were transferred to *E. coli* TG1 by P1 transduction (23). Mutant strains DSS106, DSS108, and DSS301 were constructed by the method described above, using plasmids pDMS475, pDMS450, and pDMS500, respectively (Fig. 1).

Southern blot analysis of mutants. Chromosomal DNA was prepared from putative mutant strains and TG1. Approximately 10 μg of each sample was digested to completion with *Hin*dIII, separated on a 1.2% agarose gel, transferred to

TABLE 2. Plasmids

Plasmid	Vector	Relevant information	Source or reference
pBR322		Ap^r	Pharmacia Biotechnology
pACYC184		Cm^r Tet^r	Pharmacia Biotechnology
pUC4-KIXX		Km^r	Pharmacia Biotechnology
pDMS159	pBR322	Ap^r, *dmsABC*	5
pDMS216	pBR322	Ap^r Km^r, *dmsABC*, derivative of pDMS159	5
pDMS240	pACYC184	Cm^r, *dmsABC*, derivative of pDMS216	This work
pDMS475	pBR322	Km^r, Ap^r, Δ*dmsA*, *dmsBC*, derivative of pDMS159	This work
pDMS450	pACYC184	Km^r, Cm^r, *dmsAB′-dmsC*, derivative of pDMS240	This work
pDMS500	pBR322	Ap^r, Km^r, Δ*dmsABC*, *Hin*dIII deletion of pDMSC59	This work
pDMSC59	PBR322	Ap^r, *dmsAB*, *phoA-dmsC* fusion, derivative of pDMS159	This work
pDMS350	pBR322	Ap^r, *Hin*dIII deletion of pDMS159, Δ*dmsA*, *dmsBC*	This work
pDMS355	pACYC184	Tet^r, *dmsAB′*-Δ*dmsC*, derivative of pDMS229	This work
pDMSC59X	pBR322	Ap^r, *Xho*I deletion of pDMSC59	This work
pDMS229	pTZ18R	Ap^r, *dmsABC*, derivative of pDMS216	5

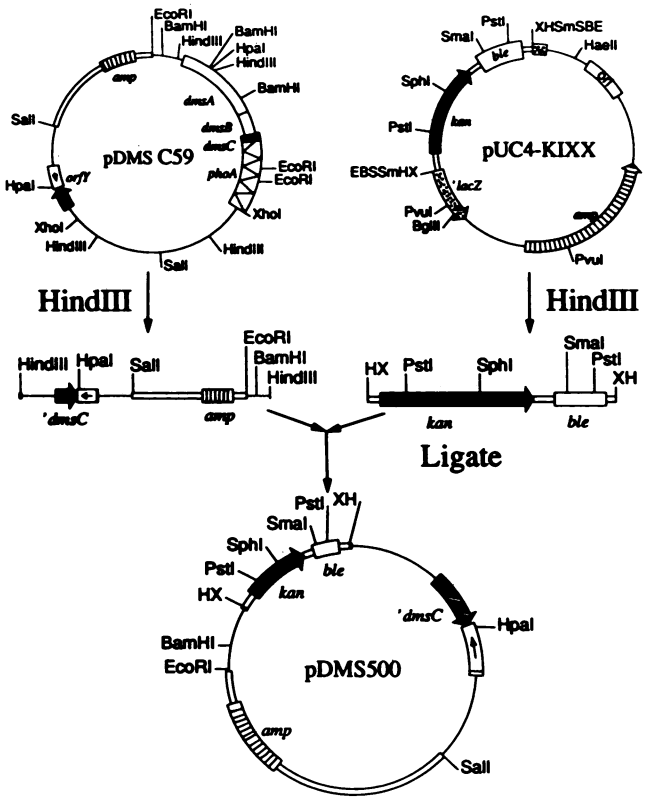

FIG. 2. Construction of recombinant plasmid pDMS500, deleted in the *dms* operon. Restriction maps of the starting plasmids pDMSC59 (17.81 kb) and pUC4-KIXX (4.0 kb) and of the derived recombinant plasmid pDMS500 are shown. See Materials and Methods for further description of pDMSC59. *Hin*dIII digestion of plasmid pDMSC59 resulted in a fragment deleted in *dmsAB* and the 5′ end of *dmsC*. This 8.05-kb (linearized) fragment carries sequences upstream of the *dms* operon (*Eco*RI-*Hin*dIII), ampicillin resistance marker from pBR322, 3′ end of *dmsC* (*dmsC′*) and downstream sequences. *Hin*dIII digestion of pUC4-KIXX generated a 1.6-kb (linearized) fragment carrying kanamycin and bleomycin resistance cartridges. Ligation of these *Hin*dIII fragments from pDMSC59 and pUC4-KIXX resulted in pDMS500 (9.65 kb). Multicloning sites in pUC4-KIXX and the fragments generated from this region abbreviated are for clarity: E, *Eco*RI; B, *Bam*HI; S, *Sac*I; Sm, *Sma*I; H, *Hin*dIII; X, *Xho*I.

BA85 nitrocellulose paper, and hybridized to a ^{32}P-labelled, nick-translated probes (*dmsABC*, *dmsA*, *dmsB*, and *dmsC* [Fig. 1]) as described previously (19). After stringent washes, the blot was exposed to X-ray film.

Preparation and analysis of plasmid DNA and transformation. Preparation, analysis, and restriction digestions of plasmid DNA were carried out as described (5, 6). All restriction enzymes and buffers were from commercial sources. Transformation of *E. coli* strains with plasmid DNA was carried out by the calcium chloride method (10).

Purification of DMSO reductase. DMSO reductase was purified from cells harboring plasmid pDMS159 as described previously (8).

Growth conditions and preparation of membrane and cytoplasmic fractions. Cultures were grown anaerobically in flasks filled to the top, using a peptone-glucose-fumarate medium (10). After 15 h at 37°C, cultures were harvested and cells were resuspended in 50 mM MOPS (pH 7.0) containing 2 mM phenylmethylsulfonyl fluoride and lysed by French

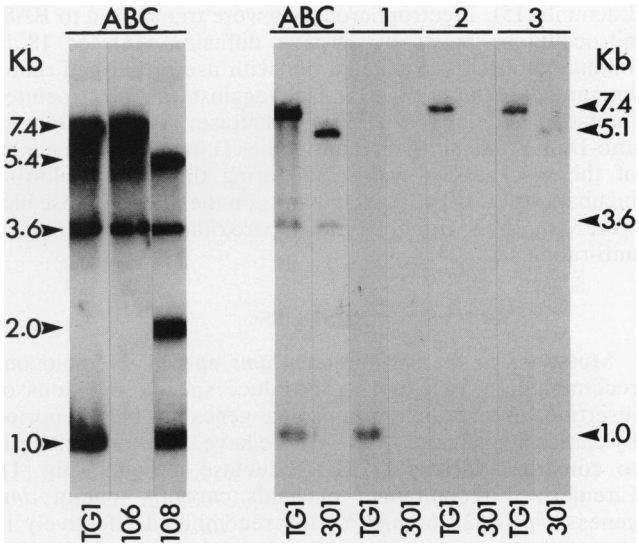

FIG. 3. Southern blot analysis of putative *dms* mutants. *Hin*dIII-digested chromosomal DNA from various strains was resolved by 1.2% agarose gel electrophoresis and transferred to nitrocellulose membranes as described in Materials and Methods. ^{32}P-labelled probes representing the entire *dms* operon together with flanking homologous chromosomal sequences (pDMS159) *dmsA* (probe 1; Fig. 1), *dmsB* (probe 2), and *dmsC* (probe 3) were used to hybridize the DNA on the filter. The horizontal bars (spanning the lanes) below each of the probes represent the analysis in corresponding individual strains (shown at the bottom). Molecular sizes of the bands are indicated.

pressure disruption at 16,000 lb/in^2. Fractionation of the lysate into membranes and cytoplasm was done as described previously (25). Membrane fractions were resuspended in the same buffer as described above. Samples were used within 3 to 5 h of preparation.

Enzyme assays. Activity of DMSO reductase was measured by monitoring the DMSO- or TMAO-dependent oxidation of reduced benzylviologen at 570 nm. The assay was carried out in 50 mM MOPS (pH 7.0) containing 0.5 mM DTT. Reactions were started by the addition of enzyme to a cuvette which contained buffer, BV (0.2 mM), dithionite (0.6 mM), and either TMAO (100 mM) or DMSO (10 mM) as a substrate. One unit of the reductase activity is defined as the amount of the enzyme which catalyzes the oxidation of 1 μmol of benzylviologen per min at 23°C. Quinol oxidase activity was measured by monitoring the reduced DMN ($DMNH_2$)- and DMSO-dependent decrease in absorbance of dithionite at 317 nm (38). The assay system for quinol oxidase contains 50 mM MOPS (pH 7.0), DTT (0.5 mM), DMSO (10 mM), dithionite (1.8 mM), and $DMNH_2$ (0.5 mM). 2-*n*-Heptyl-4-hydroxyquinolene *N*-oxide (HOQNO) was used at 6 μM. One unit of activity is defined as the amount of enzyme which catalyzes the oxidation of 1 nmol of dithionite per min at 23°C. Specific activities denote 1 U of activity per mg of protein.

Protein assay. Protein was estimated by a modification of the Lowry procedure, using bovine serum albumin as a protein standard (20).

Immunoblotting analysis and SDS-polyacrylamide gel electrophoresis. Bio-Rad mini slab gels of 12% (wt/vol) acrylamide and 0.45% (wt/vol) bisacrylamide were used. Electrophoresis was carried out at room temperature at 200 V in the discontinuous sodium dodecyl sulfate (SDS) buffer system of

Laemmli (15). Electropherograms were transferred to BA85 nitrocellulose paper by passive diffusion (16) for 18 h. Immunoblotting was carried out with use of purified rabbit immunoglobulin G (IgG) raised against the electroeluted individual subunits of DMSO reductase. A 1:1 mixture of anti-DmsA and anti-DmsB antibodies (1 mg of protein per ml of the stock IgGs) was used during the immunoblotting incubations (25). The protein bands on the nitrocellulose blot were visualized with horseradish peroxidase coupled to goat anti-rabbit IgG (24).

RESULTS

Mutations in the chromosomal *dms* operon. Homologous recombination as a tool to introduce specific deletions or insertions in targeted chromosomal genes has been reported by earlier investigators (12, 34). We have used this technique to construct various DMSO reductase mutants (Fig. 1). Circularized recombinant plasmids carrying mutant *dms* genes in pBR322 or pACYC184 recombined effectively in vivo with the homologous chromosomal regions of the *dms* operon. The recombinants selected for kanamycin resistance alone were transferred into strain TG1 by P1 transduction. A number of such mutants were analyzed by Southern blotting (Fig. 3). Each class of mutant (Fig. 1) exhibited the expected deletions or insertions which correlated with the genotype of the starting mutant plasmid. The molecular sizes of the bands were in agreement with the predicted values from the restriction map of the 20-min region of the chromosome (Fig. 1 and 3). Mutants DSS106 (Δ*dmsA*), DSS108 (*dmsAB'C*), and DSS301 (Δ*dmsABC*) were chosen for further studies.

DMSO reductase is necessary for anaerobic growth on DMSO. The deletion mutants allowed us to examine the role of the *dms* genes in anaerobic metabolism. It has been uncertain whether growth on DMSO is entirely due to the *dms* operon or whether one of the TMAO reductases (35, 38) can sustain growth on DMSO. Similarly, it was not known whether DMSO reductase accounted for the observed anaerobic growth on TMAO. The parent strain TG1 exhibited normal growth on glycerol-DMSO medium (Fig. 4A) as well as on glycerol-TMAO medium (data not shown). Mutants were grown on a minimal medium with glycerol and DMSO, TMAO, nitrate, or fumarate as the terminal electron acceptor. Mutant strains DSS301 (Fig. 4B), DSS106, and DSS108 (Fig. 4C) were unable to grow on DMSO but grew normally on TMAO (nitrate and fumarate; not shown), indicating that the *dms* operon is uniquely required for growth on DMSO and that this function cannot be filled by one of the TMAO reductases. Note that the parent strain TG1 carrying a defective plasmid, pDMS450 (*dmsAB'C*), inhibited growth on DMSO medium (Fig. 4A).

Anaerobic growth profiles of DMSO reductase mutants and in vivo complementation using *dms* plasmids. Data in Fig. 4B summarize the in vivo complementation studies carried out in DSS301. We aimed to determine which subunits are involved in the anaerobic growth of this strain on DMSO. Clearly, plasmid pDMS159, encoding all three reductase subunits, restored growth. The plasmids encoding the DmsAB (pDMSC59X), DmsAB' (pDMS355) (Fig. 4B and 5), DmsAB'C (pDMS450), and DmsBC (pDMS350) polypeptides alone were ineffective, although in each case the encoded subunits were expressed (data not shown). However, when a combination of the *dmsAB'* (pDMS355) and *dmsBC* (pDMS350) genes on two separate plasmids was introduced into this deletion strain, anaerobic growth on glycerol-DMSO medium was restored. These studies indicate that all three *dms* genes are essential to restore a positive growth phenotype. Note that expression of the truncated DmsB' along with the DmsA and DmsC subunits (pDMS450) could not restore growth.

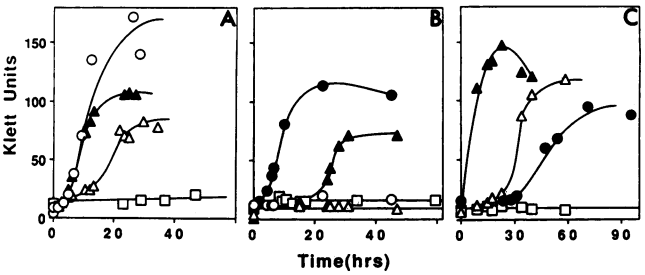

FIG. 4. Anaerobic growth profiles of various *E. coli* strains. Growth was monitored with a Klett-Summerson colorimeter equipped with a no. 66 filter. Minimal medium (5) contained 0.5% glycerol as the carbon and energy source and 70 mM DMSO or TMAO as the terminal oxidant. (A) Growth of *E. coli* DSS301 and TG1/pDMS450 (□), TG1 (△), and TG1/pDMS159 (▲) on glycerol-DMSO medium and of DSS301 on glycerol-TMAO medium (○). (B) Growth of *E. coli* DSS301 complemented with various *dms* plasmids. Growth was monitored on glycerol-DMSO minimal medium as described above. Strains carried pDMS159 (●), pDMSC59X (○), pDMS355 (□), or pDMS350 and pDMS355 (▲). △, growth profile of either pDMS450 or pDMS350. A single line was drawn for data points ○ and □ for clarity. Double transformations in DSS301 to introduce pDMS350 and pDMS355 were carried out as described earlier (10). (C) Growth of *E. coli* DSS106 and DSS108 complemented with various *dms* plasmids. Growth was monitored on glycerol-DMSO minimal medium as described above. Shown are data for DSS106 or DSS108 (□), DSS106/pDMS159 (▲), DSS106/pDMSC59X (△), and DSS108/pDMS350 (●).

In vivo plasmid complementation was also observed in strains deleted or defective in any one of the chromosomal

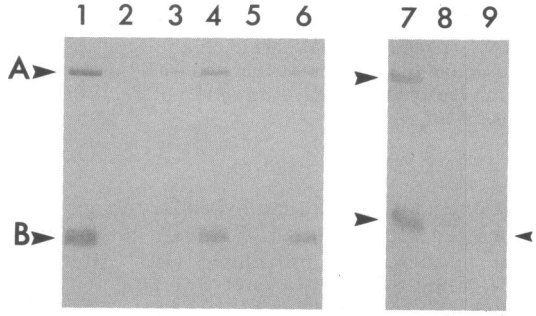

FIG. 5. Immunoblot analysis of DMSO reductase subunits of various strains grown on glucose-peptone-fumarate medium. Samples (40 μg per lane; lanes 2 to 8) were electrophoresed, immunoblotted, and stained as described in Materials and Methods. Lanes: 2 to 6, analysis from the samples indicated in Table 3; 1 and 7, 2.5 μg of purified DMSO reductase holoenzyme, with DmsA and DmsB subunits (large arrow) indicated; 2 to 5, crude membrane fractions from DSS301/pBR322, TG1, DSS301/pDMS159, and DSS301/pDMSC59X, respectively; 6, cytoplasmic fraction from strain DSS301/pDMSC59X; 8 and 9, membrane fraction (DSS106/pDMSC59X) and cytoplasmic fraction (DSS301/pDMS355), respectively, representing the samples indicated in Table 4. DmsA was not detected; DmsB' in lane 9 is indicated by the small arrow. The cytoplasmic fractions from DSS301/pDMS159 and TG1 showed the reductase subunits only at protein concentrations three- to sixfold higher than those used in this study (data not shown).

TABLE 3. Benzylviologen oxidase activities from various DMSO reductase preparations[a]

Source	Fraction	Sp act	
		DMSO	TMAO
Purified holoenzyme		91	1,049
TG1	Membranes	0.8 (63)	7.0 (58)
	Cytoplasm	0.1 (37)	1.2 (42)
DSS301/pBR322	Membranes	ND	0.13 (31)
	Cytoplasm	ND	0.08 (69)
DSS301/pDMS159	Membranes	3.0 (70)	25 (56)
	Cytoplasm	0.18 (30)	2.7 (44)
DSS301/pDMSC59X	Membranes	ND	ND
	Cytoplasm	1.41 (100)	20 (100)

[a] Purified holoenzyme was obtained as described in Materials and Methods. Cultures were grown in 250-ml flasks for 15 h at 37°C in glucose-peptone-fumarate medium. Membrane and cytoplasmic fractions were obtained as described in Materials and Methods. Reductase activities were measured with DMSO or TMAO as the substrate and reduced benzylviologen as the electron donor. Numbers in parentheses represent percent distribution of total activity. Total activities (micromoles per minute) with DMSO as the substrate are 9.2, 0, 51.2, and 75 in strains TG1, DSS301/pBR322, DSS301/pDMS159, and DSS301/pDMSC59X, respectively. When TMAO was used as a substrate, the total activity units for these strains in the same order were 98, 6.4, 532, and 1,617, respectively. Reductase specific activities are expressed as micromoles of benzylviologen oxidized per minute per milligram of protein at 23°C. ND, not detected. Data are representative of two independent experiments.

dms genes. Deletion of a 1.0-kb region in *dmsA* (DSS106) or an insertion in *dmsB* (DSS108) abolished anaerobic growth on glycerol-DMSO medium. These strains could be complemented with plasmids pDMSC59X (DmsAB) and pDMS350 (DmsBC) (Fig. 4C). Strain DSS108 could be complemented with plasmid pDMSC59X, in which a full-length DmsB is expressed (data not shown) (Table 3 and Fig. 5).

Restoration of growth characteristics in these two mutants by DmsAB/DmsBC polypeptides indicates that expression of the chromosomally encoded DmsAC (DSS108) and DmsBC (DSS106) is unaffected. These experiments indicate that different subunits of the reductase synthesized from plasmid or chromosomal genes can lead to the formation of a functional membrane-bound holoenzyme.

Cellular distribution of DMSO reductase. The DMSO reductase activity in *E. coli* TG1 (wild type) and in DSS301/pDMS159 expressing amplified holoenzyme was associated predominantly with the membrane fraction (Table 3). The *dms* deletion mutant DSS301 carrying the vector pBR322 expressed no DMSO-dependent reductase activity and very little TMAO-dependent activity. DSS301 harboring a recombinant plasmid carrying intact *dmsAB* (pDMSC59X) expressed high levels of the dimeric enzyme which totally accumulated in the cytoplasm, indicating that an intact DmsC polypeptide was required for membrane localization. The profiles of cellular distribution and the relative specific activity of the reductase remained unaffected regardless of whether DMSO or TMAO was used as the substrate in the enzyme assays. The purified holoenzyme gave a higher specific activity (11.5-fold) with TMAO than with DMSO as the substrate under these assay conditions. Similar substrate-dependent enhancement of the activity was noted in the membrane and cytoplasmic fractions derived from strains expressing DMSO reductase. Thus, in anaerobically grown *E. coli*, in the absence of inducers, DMSO reductase accounts for all the DMSO- and most of the TMAO-reducing activities of the cell.

The various reductase mutants that exhibited in vivo complementation with the *dms* plasmids were also examined for the distribution of the enzyme activity (Table 4). Clearly, the strains DSS301, DSS106, and DSS108 had no detectable reductase activities in either membrane or cytoplasmic fractions. DSS301 carrying recombinant plasmid pDMS350, encoding DmsBC, did not exhibit any reductase activity, indicating that the molybdenum-containing DmsA subunit is essential for catalytic activity. On the other hand, plasmids carrying complete *dmsAB* or *dmsAB'* lacking the C-terminal 30 amino acids of DmsB exhibited benzylviologen-mediated reductase activities localized predominantly in the cytoplasmic fraction, as expected. The deletion of *dmsC* and the region coding for C-terminal DmsB in pDMS355 (DmsAB') resulted in a reduction of the total reductase units. DSS108 complemented with pDMS350 (DmsBC) showed low reductase activities distributed almost equally in the membrane and cytoplasmic fractions. DSS301 carrying two recombinant plasmids, pDMS350 (DmsBC) and pDMS355 (Dms AB'), also produced the soluble dimeric enzyme. These results indicate that the catalytic dimer (DmsAB) when

TABLE 4. Benzylviologen oxidase activities in DMSO reductase mutants transformed with various *dms* plasmids[a]

Strain	Plasmid	Subunits	Total activity		Sp act	
			Membranes	Cytoplasm	Membranes	Cytoplasm
DSS106	None		ND	ND	ND	ND
	pDMSC59X	DmsAB	6.6 (8)	73 (92)	0.55	1.6
DSS108	None		ND	ND	ND	ND
	pDMSC59X	DmsAB	2.1 (1.8)	111.5 (97.2)	0.22	3.1
	pDMS350	DmsBC	1.1 (46)	1.3 (54)	0.1	0.04
DSS301	None		ND	ND	ND	ND
	pDMS350	DmsBC	ND	ND	ND	ND
	pDMS355	DmsAB'	0.43 (1)	33 (99)	0.05	1.8
	pDMS350 + pDMS355	DmsBC + DmsAB'	0.6 (7)	8.6 (93)	0.12	0.42

[a] Anaerobic growth of various mutants and preparations of membrane and cytoplasmic fractions were as described in the footnote to Table 3. Reductase activities were measured with benzylviologen and DMSO as electron donor and acceptor, respectively. Numbers in parentheses represent percent distribution of total activity in membrane and cytoplasmic fractions. Reductase activities and specific activities are expressed as described in Materials and Methods. ND, not detected. Data are representative of two independent experiments.

TABLE 5. Quinone oxidase activities from various DMSO reductase preparations[a]

Source	Dms subunits expressed	Fraction assayed	$DMNH_2$ oxidase sp act
Purified holoenzyme	DmsABC		1,340
TG1	DmsABC	Membranes	94
DSS301/pBR322		Membranes	<1
DSS301/pDMS159	DmsABC	Membranes	193
DSS301/pDMSC59X	DmsAB	Cytoplasm	3

[a] Purified holoenzyme, membrane, and cytoplasmic fractions from various strains were obtained as described in Materials and Methods. Quinone oxidase activity was monitored with $DMNH_2$ and DMSO as electron donor and acceptor, respectively (32). Specific activities are reported as nanomoles of dithionite oxidized per minute per milligram of protein. ND, not detected. The data are representative of two independent experiments.

overexpressed in the absence (DSS301) or in the presence of limiting amounts of DmsC (DSS106 and DSS108) accumulates in the cytoplasm. However, it is obvious that a small percentage of the trimeric membrane bound reductase expressed in vivo could still lead to the formation of a functional unit capable of supporting anaerobic growth (Fig. 4 and Table 4).

Immunoblot analysis of DMSO reductase subunits. Immunoblot analysis was used to observe the expression of the Dms polypeptides. Figure 5 shows an immunoblot of the membrane and cytoplasmic fractions from selected reductase samples (shown in Tables 3 and 4) with anti-DmsAB antibody. The membrane-bound reductase subunits of DmsA and DmsB were detected in TG1 as well as in the strain carrying the recombinant plasmids. Plasmid pDMS159 resulted in the amplification of the two subunits. The reductase subunits were also identified in the cytoplasmic fraction from the strains carrying plasmids pDMSC59X (DmsAB) and pDMS355 (DmsAB') (Fig. 5, lanes 6 and 9). The truncated DmsB' polypeptide exhibited higher electrophoretic mobility than did the full-length polypeptide. The relative band intensities were consistent with the specific activities noted for these various fractions. There was no detectable immunoreactive material in mutant strains DSS301 (Fig. 5), DSS106, and DSS108 (data not shown). Even though the cytoplasmic fraction from DSS301/pDMSC59X expressed amplified levels of the reductase subunits, the membrane fraction had no detectable immunoreactive material (Fig. 5, lane 5). The membrane fraction derived from DSS106 complemented with pDMSC59 (lane 8) also showed weak but detectable immunoreactive DmsAB subunits. Unfortunately, the DmsC subunit could not be analyzed on these blots since this polypeptide did not transfer to nitrocellulose paper under a variety of experimental conditions (25).

Catalytic properties of DMSO reductase. DMSO reductase is routinely assayed with reduced benzylviologen as an electron donor. This substrate is not related to the physiologic donor menaquinol and may distort the enzymatic mechanism. The poor solubility of menaquinol isolated from *E. coli* makes it a poor substrate for in vitro studies. To overcome these problems, we have used a soluble menaquinol analog, $DMNH_2$, as an alternate substrate in redox reactions (32). The role of the DmsC subunit in $DMNH_2$ oxidation was investigated in the trimeric holoenzyme and the dimeric soluble form of DMSO reductase. Table 5 summarizes the $DMNH_2$-mediated reductase activities with DMSO used as a substrate. The purified and the wild-type trimeric holoenzymes oxidized $DMNH_2$, whereas the soluble dimeric reductase accumulated in DSS301/pDMSC59X failed to oxidize this compound. The $DMNH_2$ oxidase activity of the trimeric enzyme was totally inhibited by the electron transfer inhibitor HOQNO. HOQNO had no inhibitory action on the benzylviologen oxidase activities. Identical results were obtained when TMAO replaced DMSO in the assay mixture, although the specific activities for the $DMNH_2$-mediated reaction were higher when TMAO was used as a substrate (data not shown). The poor activity associated with the membrane fractions in the various complementation groups listed in Table 4 prevented analysis of the $DMNH_2$ oxidase activities. These results suggest that the DmsC polypeptide is involved in the physiological electron transfer reaction from menaquinone in a manner similar to that of the anchor peptides of fumarate reductase (10, 32).

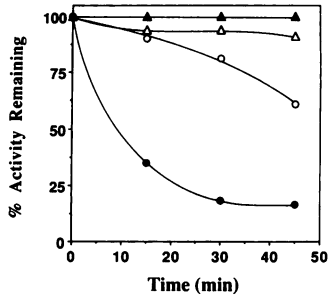

FIG. 6. Thermal inactivation of DMSO reductase. Samples were incubated at 30°C in the presence or absence of the exogenous substrate. Aliquots were withdrawn at the indicated times for measurement of the reductase activity as described in Materials and Methods, using benzylviologen and TMAO as electron donor and acceptor, respectively. Data represent purified DMSO reductase holoenzyme (▲), membrane fraction from DSS301/pDMS159 (△), and cytoplasmic fraction from DSS301/pDMSC59X in the absence (●) and presence (○) of 10 mM DMSO (or 100 mM TMAO). The contribution of DMSO carried over from the incubation mixture to the final assay mixture was negligible (<0.07 mM).

Thermostability of DMSO reductase. The role of the DmsC polypeptide in the stability of reductase activity was investigated. Figure 6 compares the thermolability of different preparations of the reductase at 30°C. The purified holoenzyme was quite stable at this temperature, as was the reductase from crude membrane fractions from both the wild type (data not shown) and the strain expressing pDMS159. The activity of the cytoplasmic fraction from DSS301/pDMSC59X was extremely labile under these conditions. The labile enzyme could be stabilized by either 100 mM TMAO or 10 mM DMSO. A number of other agents such as detergents, ethylene glycol, glycerol, EDTA, DTT, and molybdate were ineffective in stabilizing the activity of the dimeric enzyme. The dimer lost about 60% of its activity in 4 h at 4°C. Freezing in liquid nitrogen and thawing resulted in a 70% loss of activity. Again, TMAO or DMSO could stabilize the enzyme. However, these substrates could not protect the dimer for extended periods of storage or for repeated cycles of freezing and thawing. The holoenzyme was completely stable under all of these conditions.

DISCUSSION

In *E. coli*, there are several enzymes known to have DMSO- and TMAO-reducing activities (1, 28). These activities in *E. coli* were shown to be derived from an anaerobically expressed reductase encoded by the *dms* operon (3)

and by an inducible TMAO reductase encoded by the *tor* gene (28, 37). Several forms of inducible TMAO reductase have been characterized; however, antibodies raised against the major inducible, purified TMAO reductase cross-reacted with all of the inducible expressed forms. These reductases when resolved by denaturing gel electrophoresis gave a single band which exhibited specific binding with the antibodies (28). These observations provided evidence that a single TMAO reductase was expressed under inducing growth conditions. The constitutive DMSO reductase and the inducible TMAO reductase are distinct by subcellular localization and by genetic and biochemical parameters (5, 29, 36). However, the overlapping substrate specificity of these enzymes has confounded determination of the precise role of each reductase in the anaerobic electron transport chain. In vitro studies have shown that DMSO reductase can catalyze the reduction of both DMSO and TMAO (33), and this property has led to the use of the term constitutive TMAO reductase (37). We recommend that this enzyme be referred to as DMSO reductase and not as constitutive TMAO reductase to avoid further confusion in this area of research. The results presented in this and in our previous communications favor such a view. These can be summarized as follows: (i) the enzyme exhibits higher affinity for DMSO than for TMAO (5); (ii) deletion of the *dms* operon totally abolished the growth of *E. coli* on glycerol-DMSO minimal medium (Fig. 4), indicating that only DMSO reductase can utilize DMSO as the sole respiratory oxidant; (iii) deletion of the chromosomal *dms* operon also abolished the TMAO-reducing activities of the cells grown under noninducing conditions (Table 3); (iv) a *dms* deletion strain supports anaerobic growth on TMAO medium mediated by the inducible TMAO reductase (Fig. 4A); and (v) the purified, inducible TMAO reductase was shown to catalyze the reduction of only TMAO and not DMSO (38).

In *Proteus vulgaris* and *Rhodobacter* spp., a single enzyme was shown to be responsible for the reduction of TMAO and DMSO (13, 31). With the exception of the DMSO reductase in *E. coli*, all TMAO reductases studied thus far are periplasmically localized (21, 29). The pathway of electron transport to a periplasmic soluble reductase and the observed vectorial proton translocation raise questions about the mechanism of energy transduction.

The DMSO reductase from *E. coli* consistently exhibited higher specific activity when TMAO was used as a substrate (Table 3) (33). The turnover characteristics of the enzyme reducing the substrates DMSO and TMAO have also been reported to vary according to the buffer used during the assay (8). Similar observations were made with the DMSO reductase of *Rhodobacter* spp. (22, 27).

The role of the individual subunits of DMSO reductase in anaerobic respiration was clear from the in vivo complementation studies. Deletion of the entire *dms* operon or of a single gene from the chromosome destroyed the ability of *E. coli* to grow anaerobically on DMSO-containing medium. Mutants could be complemented with plasmids encoding the appropriate reductase subunits (Fig. 4). These studies indicated that all three subunits are essential for anaerobic growth on DMSO. The growth curves in Fig. 4 indicated certain interesting features. Strains expressing the complete *dms* operon on one multicopy plasmid exhibited immediate and rapid growth compared with the wild-type strain or the strains complemented with the *dms* genes (singly or in combination). The variable lag times in the growth curves are most likely due to the relatively low level of expression by the chromosomally encoded subunits (in DSS106 and DSS108) or to the overlapping regions of the *dms* operon in pDMS350 and pDMS355 affecting the assembly of the holoenzyme. A small percentage of the enzyme (Table 4) in these complemented mutant strains appear to be correctly assembled, as assessed by their ability to grow.

Complementation was achieved by deriving all three subunits from two different plasmids or by a combination of plasmid-encoded and chromosomally encoded subunits. The membrane localization of DMSO reductase was observed only in strains complemented with the entire *dms* operon (Table 3). Strains DSS106 and DSS108 complemented with plasmids encoding the DmsAB subunits resulted in the majority of expressed activity in the cytoplasm. This is to be expected since the membrane anchor subunit expressed from the chromosomal *dmsC* is limiting and cannot match the expression of catalytic DmsAB subunits from the multicopy plasmid vectors. On the other hand, DSS108 complemented with a *dmsBC* plasmid showed consistently higher distribution of the activity in the membrane fraction, approaching wild-type levels. In strain DSS301, even though both DmsAB′ and DmsBC subunits are expressed simultaneously by the multicopy vectors, the activity was predominantly in the cytoplasmic fraction (Table 4). This doubly transformed strain also expressed substantially less benzylviologen oxidase activity than did the strain in which only DmsAB′ was expressed, possibly because the truncated DmsB′ competed with the normal subunit during holoenzyme assembly.

The intensity of the reductase subunits on the immunoblots was consistent with the enzyme activity measurements (Fig. 5). The DmsB polypeptide encoded by pDMS350 was not detected on the immunoblots (at 60 μg of protein loaded on the gels) even though this plasmid in combination with pDMS355 was responsible for the positive growth phenotype in DSS301. These results imply that the majority of DmsB is rapidly degraded in the absence of the other half of the catalytic unit, DmsA. Curiously, in DSS108 the chromosomally encoded DmsAB′C did not assemble in the membrane, nor did it support the anaerobic growth of these strains on glycerol-DMSO (Fig. 4). This finding suggests that the C-terminal 30 amino acid residues of DmsB are involved in binding the anchor subunit. Expression of plasmid pDMS450, which encodes the DmsAB′C polypeptides, in *E. coli* DSS108 or TG1 resulted in the synthesis of an active dimer with >80% of the activity in the cytoplasmic fraction (data not shown). However, pDMS450 inhibited the anaerobic growth of wild-type TG1 on DMSO-containing medium (Fig. 4A). Under these conditions, expression of the modified holoenzyme, DmsAB′C, appeared to interfere with the assembly of the wild-type holoenzyme. We previously found that a mutant form of fumarate reductase, when introduced on a multicopy plasmid into wild-type *E. coli* HB101, abolished growth on glycerol-fumarate minimal medium (33).

Throughout the course of these investigations, control strain TG1 (*recA*$^+$) or its derivative mutant strains were used. The possibility of homologous recombination between the plasmid and the flanking region on the chromosome is a matter of concern in studies on in vivo plasmid complementation. Further, converting TG1 and its derivative strains to *recA* by moving the mutant *recA* gene carrying antibiotic markers by P1 transduction would pose limitations on the choice of plasmids carrying various drug resistance markers (e.g., Ap, Km, Ble, Cm, and Tet) to study in vivo complementation. To facilitate interpretation of the data, we have carried out several controls. We always adhered to stringent conditions of selection in terms of antibiotic requirements,

growth on minimal medium, and use of freshly transformed strains for growth and expression studies. The plasmid DNA (mutant or normal) could be reisolated from TG1 by standard preparative techniques. Our earlier studies on the in vivo complementation and the assembly of the fumarate reductase holoenzyme carried out in *recA* as well as *recA*$^+$ backgrounds yielded similar information (10, 17). Expression of all of the recombinant plasmids listed in Table 2 was individually verified in HB101 by enzyme activity and Western immunoblotting analysis (data not shown).

The multisubunit nature of DMSO reductase prompted us to investigate the role of individual subunits. Anaerobic reductases such as fumarate reductase and nitrate reductase have been well characterized, and their subunit functions have been identified (9, 30). The genes of these reductases (including DMSO reductase) are arranged in operons in which the order of translation is catalytic subunit-electron transfer subunit-anchor subunit (2, 7, 9). Biochemical and biophysical characterization of DMSO reductase confirmed that DmsA and DmsB are soluble catalytic and electron transfer subunits containing molybdenum cofactor and iron-sulfur centers, respectively (8). The confirmation that DmsC is the anchor verifies our topological model for the organization of DMSO reductase in the *E. coli* inner membrane (25). The artificial electron donor benzylviologen was able to mediate the reduction of DMSO in the dimeric and trimeric enzyme. Deletion of the DmsC subunit resulted in the accumulation of soluble catalytic dimer which was unable to catalyze the $DMNH_2$ oxidase reaction (Table 5). However, HOQNO, an inhibitor of in vivo electron transport, blocked the flow of electrons from $DMNH_2$ but not from benzylviologen. These observations suggest that DmsC has a quinol binding site, which may correspond to the site proposed by degli Esposti (11). This site is needed to transfer electrons to the catalytic subunits in functional electron transport. Comparison of the thermostability of the catalytic dimer with that of the holoenzyme led us to conclude that the anchor polypeptide is also necessary for the optimal stability of the catalytic dimer (Fig. 6). Thus, the DmsC subunit resembles the FrdCD subunits of fumarate reductase, which carry out identical functions. Although there is little sequence homology between the DmsC and FrdCD anchors, we have found one potentially interesting resemblance. In FrdC, His-82 appears to be necessary for quinol binding and oxidation, and it has been proposed that this residue is at the membrane interface (9). A mutation of His-82 to Arg in the sequence A-A-L-L-H-T-K-T blocks quinol oxidase activity (38). DmsC has a homologous sequence A-S-M-L-H-L-G-S between residues 61 and 68, also located at the membrane interface (2). Studies are in progress to examine the role of this histidine.

ACKNOWLEDGMENTS

This work was supported by grant MT5838 from the Medical Research Council of Canada. D.S. received support from the Alberta Heritage Foundation for Medical Research.

We thank R. B. Gennis for suggesting the mutant construction method. We also thank Catharine Trieber for providing plasmid pDMSC59 and Gillian Shaw for technical assistance.

REFERENCES

1. **Barrett, E. L., and H. S. Kwan.** 1985. Bacterial reduction of trimethylamine oxide. Annu. Rev. Microbiol. **39**:131–149.
2. **Bilous, P. T., S. T. Cole, W. F. Anderson, and J. H. Weiner.** 1988. Nucleotide sequence of the *dms ABC* operon encoding the anaerobic dimethyl-sulphoxide reductase of *Escherichia coli*. Mol. Microbiol. **2**:785–795.
3. **Bilous, P. T., and J. H. Weiner.** 1985. Dimethyl sulfoxide reductase activity by anaerobically grown *Escherichia coli* HB101. J. Bacteriol. **162**:1151–1155.
4. **Bilous, P. T., and J. H. Weiner.** 1985. Proton translocation coupled to dimethyl sulfoxide reduction in anaerobically grown *Escherichia coli* HB101. J. Bacteriol. **163**:369–375.
5. **Bilous, P. T., and J. H. Weiner.** 1988. Molecular cloning and expression of the *Escherichia coli* dimethyl sulfoxide reductase operon. J. Bacteriol. **170**:1511–1518.
6. **Birnboim, H. C., and J. Doly.** 1979. A rapid alkaline extraction procedure for screening recombinant plasmid DNA. Nucleic Acids Res. **7**:1513–1523.
7. **Blasco, F., C. Iobbi, G. Giordano, M. Chippaux, and V. Bonnefoy.** 1989. Nitrate reductase of *Escherichia coli*: completion of the nucleotide sequence of the *nar* operon and reassessment of the role of the α and β-subunits in iron binding and electron transfer. Mol. Gen. Genet. **218**:249–256.
8. **Cammack, R., and J. H. Weiner.** 1990. Electron paramagnetic resonance spectroscopic characterization of dimethyl sulfoxide reductase of *Escherichia coli*. Biochemistry **29**:8410–8416.
9. **Cole, S. T., C. Condon, B. D. Lemire, and J. H. Weiner.** 1985. Molecular biology, biochemistry and bioenergetics of fumarate reductase, a complex membrane-bound iron-sulfur flavoenzyme of *Escherichia coli*. Biochim. Biophys. Acta **811**:381–403.
10. **Condon, C., and J. H. Weiner.** 1988. Fumarate reductase of *Escherichia coli*: an investigation of function and assembly using *in vivo* complementation. Mol. Microbiol. **2**:43–52.
11. **degli Esposti, M.** 1989. Prediction and comparison of the haem-binding sites in membrane haemoproteins. Biochim. Biophys. Acta **977**:249–265.
12. **Jasin, M., and P. Schimmel.** 1984. Deletion of an essential gene in *Escherichia coli* by site-specific recombination with linear DNA fragments. J. Bacteriol. **159**:783–786.
13. **Kurihara, F. N., and T. Satoh.** 1988. A single enzyme is responsible for both dimethyl sulfoxide and trimethylamine *N*-oxide respirations as the terminal reductase in a photodenitrifier, *Rhodobacter sphaeroides* f.s. *denitrificans*. Plant Cell Physiol. **29**:377–379.
14. **Kyte, J., and R. F. Doolittle.** 1982. A simple method for displaying the hydropathic character of a protein. J. Mol. Biol. **157**:105–132.
15. **Laemmli, U. K.** 1970. Cleavage of structural proteins during the assembly of the head of bacteriophage T4. Nature (London) **227**:680–685.
16. **Latour, D. J., and J. H. Weiner.** 1987. Investigation of *Escherichia coli* fumarate reductase subunit function using transposon Tn5. J. Gen. Microbiol. **133**:597–607.
17. **Latour, D. J., and J. H. Weiner.** 1989. Assembly of *Escherichia coli* fumarate reductase holoenzyme. Biochem. Cell Biol. **67**: 251–259.
18. **Mandel, M., and A. Higa.** 1970. Calcium dependent bacteriophage DNA infection. J. Mol. Biol. **53**:159–162.
19. **Maniatis, T., E. F. Fritsch, and F. Sambrook.** 1982. Molecular cloning: a laboratory manual, p. 382–389. Cold Spring Harbor Laboratory, Cold Spring Harbor, N.Y.
20. **Markwell, M. A. K., S. M. Haas, L. L. Bieber, and N. E. Tolbert.** 1978. A modification of the Lowry procedure to simplify protein determination in membrane and lipoprotein samples. Anal. Biochem. **87**:206–210.
21. **McEwan, A. G., H. G. Wetzstein, S. J. Ferguson, and J. B. Jackson.** 1985. Periplasmic location of the terminal reductase in trimethylamine *N*-oxide and dimethylsulfoxide respiration in photosynthetic bacterium *Rhodopseudomonas capsulata*. Biochim. Biophys. Acta **806**:410–411.
22. **McEwan, A. G., H. G. Wetzstein, O. Meyer, J. B. Jackson, and S. J. Ferguson.** 1987. The periplasmic nitrate reductase of *Rhodobacter capsulatus*; purification, characterization and distinction from a single reductase for trimethylamine *N*-oxide reductase, dimethyl sulfoxide and chlorate. Arch. Microbiol. **147**:340–345.
23. **Miller, J. H.** 1972. Experiments in molecular genetics. Cold Spring Harbor Laboratory, Cold Spring Harbor, N.Y.

24. **Renart, J., J. Reiser, and G. R. Stark.** 1979. Transfer of proteins from gels to diazobenzyloxymethyl-paper and detection with antisera: a method for studying antibody specificity and antigen structure. Proc. Natl. Acad. Sci. USA **76**:3116–3120.
25. **Sambasivarao, D., D. G. Scraba, C. Trieber, and J. H. Weiner.** 1990. Organization of dimethyl sulfoxide reductase in the plasma membrane of *Escherichia coli*. J. Bacteriol. **172**:5938–5948.
26. **Sambasivarao, D., C. Trieber, C. Sedgwick, and J. H. Weiner.** Unpublished data.
27. **Satoh, T., and F. N. Kurihara.** 1987. Purification and properties of dimethyl sulfoxide reductase containing a molybdenum cofactor from a photodenitrifier, *Rhodopseudomonas sphaeroides* f.s. *denitrificans*. J. Biochem. **102**:191–197.
28. **Silvestro, A., J. Pommier, and G. Giordano.** 1988. The inducible trimethylamine *N*-oxide reductase of *Escherichia coli* K12: biochemical and immunological studies. Biochim. Biophys. Acta **954**:1–13.
29. **Silvestro, A., J. Pommier, M.-C. Pascal, and G. Giordano.** 1989. The inducible trimethylamine *N*-oxide reductase of *Escherichia coli* K12: its localization and inducers. Biochim. Biophys. Acta **999**:208–216.
30. **Stewart, V.** 1988. Nitrate respiration in relation to facultative metabolism in enterobacteria. Microbiol. Rev. **52**:190–232.
31. **Styrvold, O. B., and A. R. Strøm.** 1984. Dimethyl sulfoxide and trimethylamine oxide respiration of *Proteus vulgaris*. Evidence for a common terminal reductase system. Arch. Microbiol. **140**:74–78.
32. **Weiner, J. H., R. Cammack, S. T. Cole, C. Condon, N. Honore, B. D. Lemire, and G. Shaw.** 1986. A mutant of *Escherichia coli* fumarate reductase decoupled from electron transport. Proc. Natl. Acad. Sci. USA **83**:2056–2060.
33. **Weiner, J. H., D. P. MacIsaac, R. E. Bishop, and P. T. Bilous.** 1988. Purification and properties of *Escherichia coli* dimethyl sulfoxide, an iron-sulfur molybdo enzyme with broad substrate specificity. J. Bacteriol. **170**:1505–1510.
34. **Winans, S. C., S. J. Elledge, J. H. Krueger, and G. C. Walker.** 1985. Site-directed insertion and deletion mutagenesis with cloned fragments in *Escherichia coli*. J. Bacteriol. **161**:1219–1221.
35. **Yamamoto, I., M. Hinakura, S. Seki, Y. Seki, and H. Kondo.** 1989. Reduction of N-oxide and S-oxide compounds by *Escherichia coli*. J. Gen. Appl. Microbiol. **35**:253–259.
36. **Yamamoto, I., M. Hinakura, S. Seki, Y. Seki, and H. Kondo.** 1990. Anaerobic induction of trimethylamine *N*-oxide reductase and cytochromes by dimethyl sulfoxide in *Escherichia coli*. Curr. Microbiol. **20**:245–249.
37. **Yamamoto, I., M. Hohmura, and M. Ishimoto.** 1989. A novel gene, *tor*B, for trimethylamine *N*-oxide reductase in *Escherichia coli*. J. Gen. Appl. Microbiol. **35**:95–105.
38. **Yamamoto, I., N. Okuto, and M. Ishimoto.** 1986. Further characterization of trimethylamine *N*-oxide reductase from *Escherichia coli*, a molybdoprotein. J. Biochem. **99**:1773–1779.